

A Simple Mass Reconstruction Technique for SUSY particles at the LHC

N. Kersting¹

*Physics Department, Sichuan University
Chengdu, P.R. China 610065*

and

*Kavli Institute for Theoretical Physics China, CAS
Beijing, P.R. China 100190*

Abstract

It is often true that an invariant mass constructed from visible decay products of a heavy particle may attain a maximum(or minimum) for a certain kinematic configuration only — this fact can be used to reconstruct relevant particle masses from observed decay product momenta of events near the invariant mass endpoint. MSSM neutralino and chargino mass reconstruction at the LHC from multi-lepton endstates is illustrated by way of example.

¹nkersting@scu.edu.cn

1 Introduction

Within the first few years of LHC data collection and analysis, a key issue will not only be the search for general signs of New Physics (NP) beyond the Standard Model (SM), but also quantitative measurement of any NP particles produced. NP mass spectra, in particular, can offer an important handle on discriminating between different NP models. In the highly theoretically-motivated Minimal Supersymmetric(SUSY) Standard Model (MSSM), for example, many of the 100+ free input parameters, among which various relations are predicted by specific models of SUSY-breaking, are directly coupled to values of SUSY masses. In contrast to the situation at a lepton collider, where the center-of-mass (CM) collision energy can be precisely tuned to sweep through NP mass resonances, the LHC produces partonic collisions whose CM energies vary unpredictably from event to event, washing out potential resonance structures. Moreover, NP states may decay only partially to visible and detectable particles, as in the R-parity-conserving MSSM, where sparticles typically cascade down to SM states plus an even number of invisible Lightest SUSY Particles (LSPs). Any MSSM mass reconstruction technique applied to LHC data cannot therefore depend on the precise CM energy or total visibility of decay products.

In answer to these demands, the phenomenological community has innovated a number of different mass reconstruction methods, the most standard and well-tested among these relying on measuring endpoints of various invariant mass distributions constructed from visible final leptonic and/or jet 4-momenta [1]. In the MSSM, for example, 3-body decays of the second neutralino to a pair of leptons plus the LSP, $\tilde{\chi}_2^0 \rightarrow \ell^+ \ell^- \tilde{\chi}_1^0$, gives rise to a dilepton invariant mass distribution $M_{\ell^+ \ell^-}$ which cuts off relatively sharply at $M_{\ell^+ \ell^-}^{max} = m_{\tilde{\chi}_2^0} - m_{\tilde{\chi}_1^0}$. With a sufficiently large event sample this mass difference can be determined very precisely (to the sub-GeV level), but the values of the individual masses themselves are undetermined — this is typical of the endpoint method, where the endpoint is generally some function of a number of NP masses.

The present work introduces the idea that there can be more information at the endpoint than just its numerical value — events lying at the endpoint may arise from a unique kinematic configuration of final momenta in a decaying particle's frame — and additional analysis can be done to find the masses. Let this be defined as the DK (Decay-frame Kinematics) technique. As a first example, consider the 3-body decay noted above². An event at the dilepton endpoint must be such that, in the $\tilde{\chi}_2^0$ decay frame, the $\tilde{\chi}_1^0$ is at rest while the leptons are produced with equal and opposite momenta (the dilepton system has zero velocity). This fact allows us to find the velocity of the $\tilde{\chi}_2^0$ in the detector frame: namely, it is the observed velocity of the dilepton system, $(\vec{p}_{\ell^+} + \vec{p}_{\ell^-}) / (E_{\ell^+} + E_{\ell^-})$. When we apply the corresponding Lorentz boost to the LSP 4-vector $(m_{\tilde{\chi}_1^0}, 0, 0, 0)$ and match to observed missing transverse momenta, the LSP mass can be easily solved for — twice in fact, from each transverse direction. The fact that R-parity requires a pair of such

²The case of 2-body decays is quite similar and will be reserved for a future work [2].

decays in each event changes nothing essential: one simply finds both $\tilde{\chi}_2^0$ velocities from events at a *double-endpoint*, i.e. where both dilepton invariants are maximal, matching missing momentum to the sum of LSP momenta. Although no event ever lies exactly at a double-endpoint, a large number of events may be within a tolerably small neighborhood of it — one would expect that using these to reconstruct the LSP mass as above would give a distribution peaked at the correct value. There are, of course, immediate practical limitations — how small does the neighborhood have to be, do detector effects and backgrounds smear the peak beyond recognition, etc. — which must ultimately fall to a Monte Carlo test in order to properly address.

As a second example of the DK technique in this paper, we shall consider production of neutralino-chargino pairs $\tilde{\chi}_2^0\tilde{\chi}_1^\pm$ in the MSSM, with subsequent decays $\tilde{\chi}_2^0 \rightarrow \ell^+\ell^-\tilde{\chi}_1^0$ and $\tilde{\chi}_1^\pm \rightarrow \ell^\pm\nu\tilde{\chi}_1^0$. Though slightly more complicated than the case of neutralino-pair decays, the same principle works: events at a particular endpoint belong to a certain class of kinematics in the $\tilde{\chi}_2^0$ and $\tilde{\chi}_1^\pm$ decay frames, allowing us to find the individual velocities of these latter; the LSP 4-momenta can then be boosted and matched to observed missing momentum for only one (correct) value of the chargino mass.

The structure of this work will be as follows: Section 2 will illustrate the DK technique in more detail in the case of neutralino-pair production, where the goal is LSP mass-reconstruction — this includes a Monte Carlo simulation to test how well the technique might actually work with LHC data. Section 3 then does the same for neutralino-chargino pair production, again seeing how well the chargino mass can be reconstructed. Section 4 summarizes these results, comments on the relation to other mass reconstruction techniques in the literature, and discusses general applicability.

2 Neutralino-Neutralino Modes

2.1 Theory

Consider production of neutralino pairs in the MSSM which undergo 3-body decays to electrons and muons:

$$pp \rightarrow \mathbb{X} \rightarrow \mathbb{X}' + \tilde{\chi}_i^0 (\rightarrow e^+e^-\tilde{\chi}_1^0) \tilde{\chi}_j^0 (\rightarrow \mu^+\mu^-\tilde{\chi}_1^0) \quad (1)$$

where \mathbb{X} represents either Z^* or any MSSM production channel from a Higgs (H^0 or A^0) or colored gluino/squark cascades, while \mathbb{X}' are SM states potentially produced in association, all irrelevant to the current discussion; note we could include $e^+e^-e^+e^-$ and $\mu^+\mu^-\mu^+\mu^-$ endstates as well, but at the price of a two-fold ambiguity in lepton pairing in what follows. Physical observables from one event thus consist of four leptonic 4-momenta p_{e^\pm,μ^\pm} (from which we may construct the usual dilepton invariant masses, M_{ee} and $M_{\mu\mu}$) and missing momentum in two transverse directions, assumed equal to the sum of the two $\tilde{\chi}_1^0$'s' transverse momenta, $p_{1,2}^T$. Decay kinematics (see Appendix) allow us to write the following list of constraints on the relevant neutralino

masses (hereafter we abbreviate $m_i \equiv m_{\tilde{\chi}_i^0}$):

$$|\vec{p}'_{e^+} + \vec{p}'_{e^-}| = \frac{1}{2m_i} \sqrt{(M_{ee}^2 - m_1^2 - m_i^2)^2 - 4m_1^2 m_i^2} \quad (2)$$

$$|\vec{p}'_{\mu^+} + \vec{p}'_{\mu^-}| = \frac{1}{2m_j} \sqrt{(M_{\mu\mu}^2 - m_1^2 - m_j^2)^2 - 4m_1^2 m_j^2} \quad (3)$$

$$(\vec{p}_1 + \vec{p}_2)^T = \vec{p}^T \text{ (observed)} \quad (4)$$

where leptonic momenta are written in the frame of the respective parent neutralino, i.e. $p'_{e^\pm} = \Lambda_1 p_{e^\pm}$ and $p'_{\mu^\pm} = \Lambda_2 p_{\mu^\pm}$, defining the appropriate Lorentz transformations $\Lambda_{1,2}$. In general, of course, we do not know the Lorentz boosts $\vec{\beta}_{1,2}$ from which $\Lambda_{1,2}$ are constructed, so (2)-(4) represents a system of four equations (or six, if the dilepton endpoints $M_{\ell\ell}^{max} = m_{i,j} - m_1$ are known) for nine unknowns ($\vec{\beta}_{1,2}$ and the masses $m_{1,i,j}$) which obviously cannot be solved uniquely for the masses.

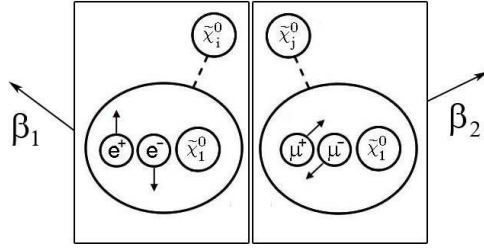


Figure 1: *An event with maximal M_{ee} and $M_{\mu\mu}$: though the decaying neutralinos $\tilde{\chi}_{i,j}^0$ may be moving with any velocity $\beta_{1,2}$ in the lab frame, in each respective decay frame the leptons have equal and opposite momenta while the $\tilde{\chi}_1^0$ is at rest.*

Supposing, however, we have an event where the invariant masses M_{ee} and $M_{\mu\mu}$ are maximal, as in Fig. 1, an enlarged system of constraints results:

$$M_{ee} = m_i - m_1 \quad (5)$$

$$M_{\mu\mu} = m_j - m_1 \quad (6)$$

$$|\vec{p}'_{e^+} + \vec{p}'_{e^-}| = 0 \quad (7)$$

$$|\vec{p}'_{\mu^+} + \vec{p}'_{\mu^-}| = 0 \quad (8)$$

$$(\vec{p}_1 + \vec{p}_2)^T = \vec{p}^T \text{ (observed)} \quad (9)$$

which now gives ten equations ((7) and (8) stand for three constraints each) for the nine unknowns³, allowing us to actually overconstrain the masses $m_{1,i,j}$. The $\vec{\beta}_{1,2}$ which satisfy (7) and (8), making the total momentum of each lepton pair zero, are uniquely given by

$$\vec{\beta}_1 = \frac{\vec{p}_{e^+} + \vec{p}_{e^-}}{E_{e^+} + E_{e^-}} \quad \vec{\beta}_2 = \frac{\vec{p}_{\mu^+} + \vec{p}_{\mu^-}}{E_{\mu^+} + E_{\mu^-}} \quad (10)$$

³Strictly speaking, there is a two-fold ambiguity between (5) and (6), unless $i = j$.

Now the corresponding $\Lambda_{1,2}$ which take the $e^+e^-\tilde{\chi}_1^0$ and $\mu^+\mu^-\tilde{\chi}_1^0$ systems to their respective $\tilde{\chi}_{i,j}^0$ -rest frames also bring each $\tilde{\chi}_1^0$ to rest (a condition of M_{ee} and $M_{\mu\mu}$ being maximal): their 4-momenta in these frames must thus be $(m_1, \vec{0})$, which, when inverse-Lorentz-transformed by $\Lambda_{1,2}^{-1}$ to give $(m_1\gamma_{1,2}, m_1(\vec{\beta}\gamma)_{1,2})$, must agree with the observed missing momentum \vec{p}^T ; a matching condition along each transverse direction (say \hat{x} and \hat{y}) then gives two independent determinations of m_1 :

$$m_1' = \frac{\vec{p}_x}{(\beta_x\gamma)_1 + (\beta_x\gamma)_2} \quad m_1'' = \frac{\vec{p}_y}{(\beta_y\gamma)_1 + (\beta_y\gamma)_2} \quad (11)$$

Since we are assuming that both M_{ee} and $M_{\mu\mu}$ are precisely maximal (the perfect event of Fig. 1), we would of course get $m_1' = m_1'' = m_1$; in practice, of course, we can only expect to capture an event within some neighborhood ϵ of the endpoints, $M_{ee,\mu\mu} = M_{ee,\mu\mu}^{max} \pm \epsilon$, in which case one can show (see Appendix) that m_1' and m_1'' are approximately $\sim m_1 \pm \sqrt{2\epsilon m_1}$. One might then expect that applying (10) and (11) to a sample of events near the endpoint should give a distribution of m_1' and m_1'' peaked near m_1 with a $O(\sqrt{2\epsilon m_1})$ spread; we will presently see that a Monte Carlo simulation, adding in experimental effects such as measurement errors and inherent finiteness of detector resolution, as well as the inclusion of SM and MSSM backgrounds, basically confirms this expectation.

2.2 Monte Carlo Test

In order to see how well the above programme might work with real data, let us apply it to Monte Carlo simulated LHC data, choosing for definiteness the following MSSM parameter point:

$$\begin{aligned} \mu &= 390 \text{ GeV} & \tan\beta &= 10 & m_A &= 400 \text{ GeV} \\ M_1 &= 100 \text{ GeV} & M_2 &= 123 \text{ GeV} & m_{\tilde{g}} &= 605 \text{ GeV} \\ m_{\tilde{q}} &= 500 \text{ GeV} & m_{\tilde{\ell}_{L,\tilde{\tau}}} &= 300 \text{ GeV} & m_{\tilde{\ell}_R} &= 130 \text{ GeV} \end{aligned}$$

which is a modification of the SPS1a' benchmark point [3] enhancing the $\tilde{\chi}_2^0 \rightarrow \ell^+\ell^-\tilde{\chi}_1^0$ branching ratio.

Colored sparticles, dominating the bulk of the inclusive SUSY cross section ($\sim 70 \text{ pb}$) at this point, cascade predominantly to $\tilde{\chi}_2^0$ ($\sim 30\%$) or $\tilde{\chi}_1^\pm$ ($\sim 60\%$), excepting R-handed squarks (which mostly decay directly to the LSP). As can be seen from the gaugino mass spectrum in Table 1, the mass splitting between $\tilde{\chi}_2^0$ and $\tilde{\chi}_1^0$ (the LSP) of $m_2 - m_1 = 18.7 \text{ GeV}$ is too small to allow anything but $\tilde{\chi}_2^0$ decay through an off-shell intermediary (slepton or Z^*) as desired: $\tilde{\chi}_2^0 \rightarrow \ell^+\ell^-\tilde{\chi}_1^0$ has $BR \approx 90\%$ (next of importance is $\tilde{\chi}_2^0 \rightarrow qq'\tilde{\chi}_1^0$ with $BR \approx 9\%$). SUSY $e^+e^-\mu^+\mu^-$ endstates should therefore arise almost entirely from $\mathbb{X} \rightarrow \mathbb{X}' + \tilde{\chi}_2^0 (\rightarrow e^+e^-\tilde{\chi}_1^0) \tilde{\chi}_2^0 (\rightarrow \mu^+\mu^-\tilde{\chi}_1^0)$.

Proton-proton collisions corresponding to 100 fb^{-1} of LHC luminosity are then generated with HERWIG 6.5 [4] (coupled to the CTEQ6 parton distribution functions [5]) for all relevant SUSY processes ($pp \rightarrow$ any pair of $\{\tilde{q}, \tilde{g}, \tilde{\chi}^\pm, \tilde{\chi}^0\}$, $pp \rightarrow \tilde{\ell}\tilde{\ell}$)

Table 1: *Gaugino masses (in GeV) at the MSSM parameter point considered.*

$\tilde{\chi}_1^0$	$\tilde{\chi}_2^0$	$\tilde{\chi}_3^0$	$\tilde{\chi}_4^0$	$\tilde{\chi}_1^\pm$	$\tilde{\chi}_2^\pm$
96.5	115.2	393.8	404.9	114.2	406.0

and SM backgrounds (for a hard 4-lepton signal only $Z^{(*)}Z$ is sizeable [6]), coupled to a simplified detector simulator⁴ which only passes events with four hard, isolated⁵ leptons with flavor structure $e^+e^-\mu^+\mu^-$. The wedgebox plot of Fig. 2a shows all surviving events (~ 5000 of these) by position in $(M_{ee}, M_{\mu\mu})$ -space and is well-suited to picking out those arising from the desired $\tilde{\chi}_i^0\tilde{\chi}_j^0$ -origin [9]; in this case the dense box-like structure in the corner ($M_{ee,\mu\mu} < 20$ GeV) arises from $\tilde{\chi}_2^0\tilde{\chi}_2^0$ -pair decays as expected; areas of the wedgebox plot not relevant to the present study include the ‘wings’ projecting along either axis, arising from decays of more sparsely-produced $\tilde{\chi}_2^0\tilde{\chi}_{3,4}^0$ and $\tilde{\ell}\tilde{\ell}$ pairs, as well as the two lines of points concentrated around $M_{ee,\mu\mu} \approx 90$ GeV due to the $Z^{(*)}Z$ background.

Focusing on the corner region then, a flavor-subtracted dilepton invariant mass distribution (Fig. 2b) constructed from hard 2-lepton events (over 27000 of these) is most useful for pinpointing the endpoint: for our purposes it is enough to roughly identify $M_{\ell^+\ell^-}^{max} \approx 19$ GeV by visual inspection (this is already in excellent agreement with the expected value of $m_2 - m_1 = 18.7$ GeV). Note the less-than-triangular shape of this distribution does indicate the 3-body nature of the $\tilde{\chi}_2^0$ -decays responsible. The $\tilde{\chi}_2^0\tilde{\chi}_2^0$ box on the wedgebox plot is of course defined where $M_{ee,\mu\mu} < M_{\ell^+\ell^-}^{max}$, and an enlarged view of this region (Fig. 2c) allows us to select an event sample in the neighborhood of $M_{ee,\mu\mu} \sim M_{\ell^+\ell^-}^{max}$ — here ‘neighborhood’ might be defined as $M_{\ell^+\ell^-}^{max} - \epsilon < M_{ee,\mu\mu} < M_{\ell^+\ell^-}^{max}$ for some optimal ϵ , i.e. ϵ must be large enough to get more than a few events, yet not so large that the kinematic configuration of Fig. 1 becomes a bad approximation for most events; at the present point $\epsilon = 2$ GeV seems best (see below), giving an event sample of size $O(10^2)$. For each such event, (10) and (11) are applied from the measured leptonic momenta and missing transverse momenta, both m' and m'' being added to the final distribution (Fig. 2d) only if they agree with each other to within 20% — this is very effective at eliminating not only background events which by chance might fall in the sampling region, but also legitimate $\tilde{\chi}_2^0\tilde{\chi}_2^0$ events for which the DK technique would fail (mostly because of momentum mis-measurement effects in the detectors but also possibly from wrongly-assumed kinematics of Fig. 1) — nevertheless, some events give consistent solutions which lie far from the prominent peak at 80–100 GeV. At any rate, a Gaussian fit⁶ to

⁴An identical set-up was employed in the author’s previous publications [7, 8] and the reader is referred there for additional details.

⁵No tracks of other charged particles are present in a $r = 0.3$ rad cone around the lepton, with less than 3 GeV of energy deposited into the electromagnetic calorimeter for 0.05 rad $< r < 0.3$ rad, and $p_T^\ell > 10, 8$ GeV for $\ell = e, \mu$.

⁶For lack of a known theoretical shape. Away from the peak the distribution is clearly non-Gaussian, a feature which the author has found true at other parameter points tested.

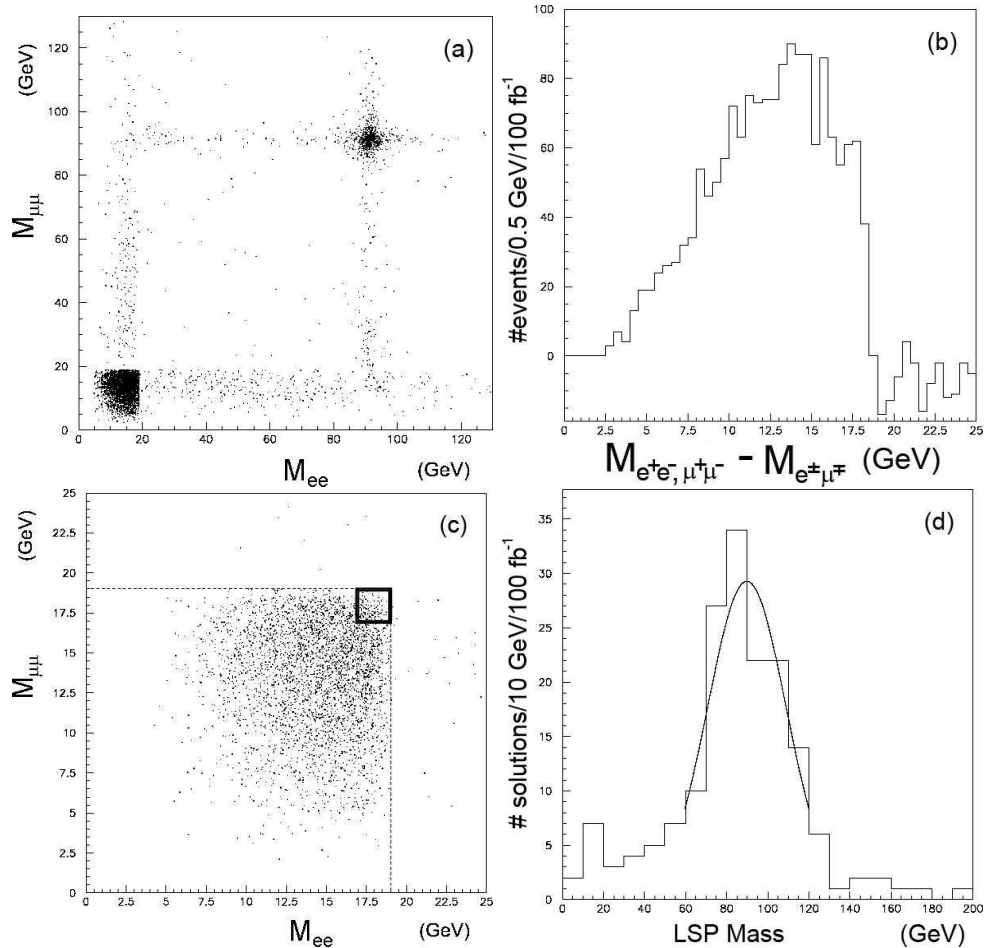


Figure 2: (a) Wedgebox plot (100 fb^{-1}) showing a very dense box with diffuse backgrounds (except near the Z-pole). (b) Flavor-subtracted dilepton events give a sharp distribution with an edge of approximately $M_{\ell^+\ell^-}^{\text{max}} \approx 19 \text{ GeV}$. (c) Enlarged view of the wedgebox within this edge; events for analysis are taken from the small boxed region of area $2 \times 2 \text{ GeV}^2$ shown. (d) Distribution of reconstructed LSP mass, with Gaussian fit overlaid: $m_{\tilde{\chi}_1^0} = 89.9 \pm 19.1 \text{ GeV}$.

the peak indicates a reconstructed LSP mass of $m_1 = 89.9 \pm 19.1 \text{ GeV}$, in safe agreement with the nominal value in Table 1. The slight downwards bias in the central value seems to be a systematic effect, for increasing ϵ enhances the bias — indeed, at lower ϵ (selecting a sample of events more closely approximating the kinematics of Fig. 1) the central value more closely approaches the nominal one, but at the price of statistics, the balancing of these two effects leading to the quoted value of $\epsilon = 2 \text{ GeV}$. Recall from the theoretical discussion above that the expected width of the LSP-mass distribution would then be at least $O(\sqrt{2\epsilon m_1}) = O(\sqrt{(2)(2)(90)}) \text{ GeV} \approx 19 \text{ GeV}$, in good agreement with what is seen; a higher luminosity sample (even at full design luminosity of 300 fb^{-1}) might permit a smaller optimal ϵ , say $\epsilon \sim 1 \text{ GeV}$, but the distribution width of $\sqrt{2\epsilon m_1}$ would not be expected to decrease significantly — application of DK therefore reliably locates the LSP mass, but only to a limited precision

(probably 10% at best). This may, nevertheless, be entirely sufficient for discriminating among different SUSY models, and, as we shall see next, is also good enough to find the mass of the lighter chargino.

3 Neutralino-Chargino Modes

The foregoing has demonstrated how the DK technique reconstructs the LSP mass from 4-lepton endstates of neutralino pair ($\tilde{\chi}_2^0\tilde{\chi}_2^0$) decays; let us now see how DK also reconstructs the chargino mass from 3-lepton endstates of neutralino-chargino ($\tilde{\chi}_2^0\tilde{\chi}_1^\pm$) decays, again taking these to be through off-shell intermediates, i.e.

$$pp \rightarrow \mathbb{X} \rightarrow \mathbb{X}' + \tilde{\chi}_2^0 (\rightarrow e^+ e^- \tilde{\chi}_1^0) \tilde{\chi}_1^\pm (\rightarrow \mu^\pm \nu \tilde{\chi}_1^0) \quad (12)$$

or with $e \leftrightarrow \mu$; again, same-flavor endstates such as $e^+e^-e^\pm$ or $\mu^+\mu^-\mu^\pm$ could also be included in this analysis at the price of a two-fold ambiguity in lepton-pairing.

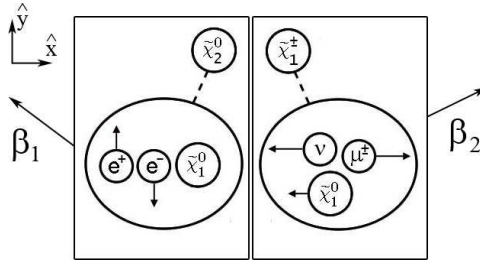


Figure 3: *Events of interest for reconstructing the chargino mass: in the frame where the $\tilde{\chi}_2^0$ decays at rest, the e^\pm are along some global coordinates $\pm\hat{y}$ with maximal energy; likewise in the $\tilde{\chi}_1^\pm$ decay frame the muon is along $\pm\hat{x}$ with maximal energy. The velocities $\beta_{1,2}$ are a priori unknown.*

With the $\tilde{\chi}_2^0\tilde{\chi}_2^0$ modes of the last section, it was natural to classify 4-lepton events by their dilepton invariant masses $M_{ee,\mu\mu}$ in the form of a wedgebox plot, events of interest being concentrated near $M_{ee} = M_{\mu\mu} = M_{\ell\ell}^{max}$. Here with 3-lepton events, a natural way to classify events is by the dilepton invariant M_{ee} and the invariant \overline{M}_{l2l} , defined as

$$\overline{M}_{l2l}^4 \equiv \{(p_{e^+} + p_{e^-} - p_{\mu^\pm})^4 + (p_{\mu^\pm} + p_{e^+} - p_{e^-})^4 + (p_{e^-} + p_{\mu^\pm} - p_{e^+})^4\}/3 \quad (13)$$

since, as found in [7], events with maximal $M_{ee} = M_{\ell\ell}^{max}$ and minimal \overline{M}_{l2l} arise from events as shown in Fig. 3, i.e. if the decaying $\tilde{\chi}_2^0$ and $\tilde{\chi}_1^\pm$ had no motion then the e^\pm would have equal and opposite momenta (along say $\pm\hat{y}$) while the muon would be emitted perpendicular to \hat{y} , say along \hat{x} , also with maximal kinetic energy.

Just as before, the required Lorentz transformation Λ_1 to get the e^+e^- pair in the frame of the decaying neutralino ($p'_{e^\pm} = \Lambda_1 p_{e^\pm}$) is determined by

$$\vec{\beta}_1 = \frac{\vec{p}_{e^+} + \vec{p}_{e^-}}{E_{e^+} + E_{e^-}} \quad (14)$$

There is unfortunately no such simple formula for $\vec{\beta}_2$, but it is nevertheless uniquely defined by the following system of equations describing conservation of the total missing 4-momentum \not{p}^μ ,

$$\not{p}^\mu = \Lambda_1^{-1} \begin{pmatrix} m_1 \\ \vec{0} \end{pmatrix} + \Lambda_2^{-1} \begin{pmatrix} m_\pm - E'_{\mu^\pm} \\ -\vec{p}'_{\mu^\pm} \end{pmatrix} \quad \left[\begin{array}{l} \left(\begin{array}{c} E'_{\mu^\pm} \\ \vec{p}'_{\mu^\pm} \end{array} \right) \equiv \Lambda_2 \left(\begin{array}{c} E_{\mu^\pm} \\ \vec{p}_{\mu^\pm} \end{array} \right) \\ m_\pm \equiv m_{\tilde{\chi}_1^\pm} \end{array} \right] \quad (15)$$

of which the two transverse components \vec{p}'^T are measurable, in addition to the three kinematic constraints

$$\vec{p}'_{e^\pm} \cdot \vec{p}'_{\mu^\pm} = 0 \quad , \quad E'_{\mu^\pm} = \frac{m_\pm^2 - m_1^2}{2m_\pm} \quad , \quad M_{ee} = m_2 - m_1 \quad (16)$$

which events of the form shown in Fig. 3 must obey. Thus, (15) and (16) compose a system of five equations for the six unknowns $\{\vec{\beta}_2, m_1, m_2, m_\pm\}$. Supposing m_1 is already determined (say from the last section), then we are less one unknown and the chargino mass m_\pm can found from one (perfect) event, in principle. The usual practical caveats apply to this claim, so again we will have to check via Monte Carlo.

3.1 Monte Carlo Test

Working with the same MSSM parameter point and Monte Carlo setup as in the last section, signal and background processes (now including significant 3-lepton sources such as $W\gamma^*/Z$) for 100 fb^{-1} integrated luminosity are generated and now filtered for events with only three hard and isolated leptons — this, in addition to the fact that squark BR's to charginos are typically twice those to neutralinos at this point, gives a much larger signal: the “ $M_{\ell+\ell-}$ versus \overline{M}_{l2l} ” plot of Fig. 4a represents well over $4 \cdot 10^4$ events. Though this plot gives us some discriminating power between signal and background, e.g. the majority of SM background events cluster about the line $M_{\ell+\ell-} = m_Z$ (cut off by the plot), there is still a more-or-less uniform distribution of background events such as $\tilde{\chi}_2^0 \tilde{\chi}_1^\pm (\rightarrow \tau \nu \tilde{\chi}_1^0)$ (the tau decaying leptonically) which will have to be tolerated.

From the previous theoretical discussion we know where to look on this plot, viz. the small rectangular box in Fig. 4a containing events assumed to be of the type shown in Fig. 3: by trial and error it is found that the several hundred events here satisfying $M_{\ell+\ell-} = 18 \pm 1$ GeV and $\overline{M}_{l2l} < 20$ GeV give an optimal sample in the sense discussed above in Section 2. For each such event, m_1 is chosen in the interval $m_1 = 89.9 \pm 19.1$ GeV (flat priors) and the system of equations (14)-(16) is solved for m_\pm . Only physical solutions (m_\pm is real and $> m_1$) are kept and plotted in Fig. 4b. A Gaussian fit to the peak gives $m_\pm = 106.2 \pm 11.6$ GeV, in good agreement with the actual value $m_\pm = 114.2$ GeV; note again, however, the downwards bias in the central value. As with the fit to the LSP mass in the last Section, repeating the analysis with various smaller-sized sampling regions decreased the bias at the cost of statistics, so this is understood to be a systematic uncertainty of DK.

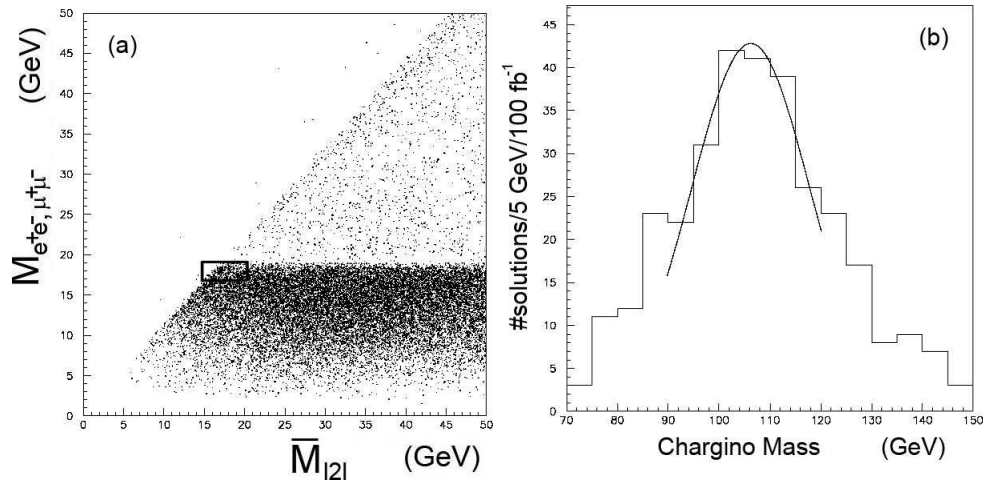


Figure 4: (a) Correlation between $M_{\ell^+\ell^-}$ and \bar{M}_{l2l} (100 fb^{-1}); events are taken in the boxed region shown where $M_{\ell^+\ell^-} = 18 \pm 1 \text{ GeV}$ and $\bar{M}_{l2l} < 20 \text{ GeV}$. (b) Distribution of reconstructed chargino mass from events in this boxed region, assuming the reconstructed LSP mass of $m_1 = 89.9 \pm 19.1 \text{ GeV}$. A Gaussian fit gives $m_{\tilde{\chi}_1^\pm} = 106.2 \pm 11.6 \text{ GeV}$.

4 Discussion and Summary

We have now seen two specific examples in the MSSM (from $\tilde{\chi}_2^0\tilde{\chi}_2^0$ and $\tilde{\chi}_2^0\tilde{\chi}_1^\pm$ pair decays) of how DK operates: events near the endpoint of a particular invariant mass distribution (in the black boxes of Figs. 2c and 4a, respectively) can be used to reconstruct masses (m_1 and m_\pm) to reasonable ($\sim 10 - 20\%$) precision, at least with the LHC luminosity and MSSM input parameters assumed here. Though 3-body decays $\tilde{\chi}_2^0 \rightarrow \ell^+\ell^-\tilde{\chi}_1^0$ and $\tilde{\chi}_1^\pm \rightarrow \mu^\pm\nu\tilde{\chi}_1^0$ were assumed for the sake of simplicity, the DK technique also works (with minor adjustments) for 2-body decays through on-shell sleptons [2].

It is important to ask how this technique performs relative to other mass reconstruction methods available (excepting, of course, the traditional endpoint-value method, which is incorporated into DK). First consider the reconstruction of neutralino masses. There are now an array of methods which take advantage of the pair-production of neutralinos. One class of “Mass-Shell Techniques” (MST), represented in the work of [10] and [11], essentially depends on maximizing the solvability of assumed mass-shell constraints in a given sample of events. This seems quite effective for on-shell decays⁷, but for the off-shell decay topologies in the present work these methods cannot be applied since there are not enough such constraints. Recently fashionable “transverse mass variable” methods [12, 13], e.g. m_{T2} , might be applied; in one such development [14], for example, a “constrained mass variable” m_{2C} proves quite powerful for $\tilde{\chi}_2^0\tilde{\chi}_2^0$ modes (also assuming 3-body decays $\tilde{\chi}_2^0 \rightarrow \ell^+\ell^-\tilde{\chi}_1^0$). In any case, if any of the above methods are applicable, they should perform much better than DK alone, since all $\tilde{\chi}_2^0\tilde{\chi}_2^0$ events (not just those close to a double-endpoint) are

⁷But see [9] for some important caveats.

used. As for decay modes with charginos, such as the $\tilde{\chi}_1^\pm \tilde{\chi}_2^0$ modes considered in this work, it would seem that other techniques would encounter difficulties due to extra invisible particles (neutrinos) in the decay products. There is the interesting prospect, however, of somehow conjoining these techniques with DK for a better fit of the chargino mass.

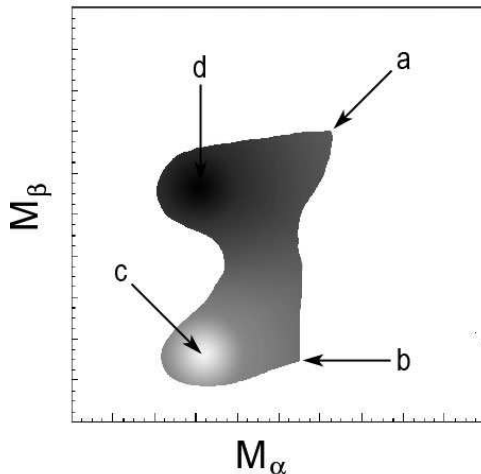


Figure 5: *General 2d Dalitz plot; (a)-(d) indicate special regions which may have unique kinematics applicable to DK analysis.*

The DK technique is by no means limited to neutralino or chargino decays, nor just to MSSM applications. Any NP decay chain which is subject to the traditional invariant mass endpoint method also can be analyzed with DK. The key is to choose invariant masses whose endpoints correspond to unique decay-frame kinematics, e.g. $M_{\ell\ell}$ (at its maximum) in the case of neutralino decays, or both $M_{\ell\ell}$ and \overline{M}_{l2l} (which must be simultaneously maximal and minimal, respectively) for neutralino-chargino decays. This statement allows one to imagine how the DK technique might work in general: depending on the specific number and type of invariant masses one can construct from the endstates of a given decay chain, some d -dimensional Dalitz plot of these will be useful for isolating events with a unique decay-frame kinematic configuration. Fig. 5 shows, for example, a hypothetical 2d Dalitz plot of some invariants M_α and M_β : points which might exhibit unique, identifiable decay-frame kinematics, hence amenable to DK analysis, include (a)extrema⁸, (b)kinks, (c)internal density minima or (d)maxima. Extension to $d \geq 3$ - dimensional Dalitz plots is feasible if enough events can be collected to fill in the shape.

Acknowledgements

This work was funded in part by the Kavli Institute for Theoretical Physics (Beijing).

⁸But beware: endpoints do not always arise from unique kinematic configurations; see [8].

Appendix

Off-Shell Kinematics

Consider the three-body decay $\tilde{\chi}_i^0 \rightarrow \ell^+ \ell^- \tilde{\chi}_1^0$ in the rest frame of the decaying neutralino. Working in the approximation where the lepton mass is zero, the leptonic four-momenta are $p_{\ell^\pm}^\mu = (E_\pm, E_\pm \hat{p}_\pm)$ and the dilepton invariant mass $M_{\ell^+ \ell^-}^2 \equiv (E_+ + E_-)^2 - (E_+ \hat{p}_+ + E_- \hat{p}_-)^2$ can be rewritten as

$$M_{\ell^+ \ell^-}^2 = 2E_+ E_- (1 - \cos\theta) \quad (17)$$

where θ is the angle between the leptons. Energy and momentum conservation further imply

$$E_+ + E_- + E_1 = m_i \quad (18)$$

$$E_+ \hat{p}_+ + E_- \hat{p}_- + \vec{p}_1 = 0 \quad (19)$$

where the four vectors of the $\tilde{\chi}_{1,2}^0$ in this frame are (E_1, \vec{p}_1) and $(m_i, \vec{0})$, respectively. Equations (17)-(19) give

$$|E_+ \hat{p}_+ + E_- \hat{p}_-| = \frac{\sqrt{(M_{\ell^+ \ell^-}^2 - m_1^2 - m_i^2)^2 - 4m_1^2 m_i^2}}{2m_i} \quad (20)$$

which in the limit where $M_{\ell^+ \ell^-}$ attains its maximum ($= m_i - m_1$) reduces to

$$|E_+ \hat{p}_+ + E_- \hat{p}_-| = 0 \quad (21)$$

further implying

$$E_\pm = \frac{m_i - m_1}{2} \quad (22)$$

$$\cos\theta = -1 \quad (23)$$

i.e. the one constraint (20) is replaced by (21)-(23) for events with maximal dilepton invariant mass.

Spread of LSP mass measurement

In the discussion of Section 2 we showed that if we have the perfect event $M_{ee} = M_{\mu\mu} = M_{\ell\ell}^{max}$ then the extracted masses in (11) both give $m'_1 = m''_1 = m_1$. In a finite-size event sample we can only expect to approach perfection, say $M_{ee, \mu\mu} = M_{\ell\ell}^{max} - \epsilon$. In this case the Lorentz transforms defined in (10) will not give the LSP rest frames, where by definition their energies are $E_{1,2} = m_1$, but rather frames where

$$E_{1,2} = \frac{M_{ee, \mu\mu}^2 - m_1^2 - m_i^2}{2m_i} \approx m_1 + \epsilon \left(1 - \frac{m_1}{m_i}\right) \quad (24)$$

as can be derived from (17)-(19) above, with corresponding momenta

$$|\vec{p}_{1,2}| \approx \sqrt{2\epsilon m_1 \left(1 - \frac{m_1}{m_i}\right)} \quad (25)$$

Inverse-Lorentz-transforming *these* four-vectors gives

$$p_{1,2}^\mu = \begin{pmatrix} \gamma & \beta_x \gamma & \beta_y \gamma & \beta_z \gamma \\ \beta_x \gamma & 1 + (\gamma - 1) \frac{\beta_x^2}{\beta^2} & (\gamma - 1) \frac{\beta_x \beta_y}{\beta^2} & (\gamma - 1) \frac{\beta_x \beta_z}{\beta^2} \\ \beta_y \gamma & (\gamma - 1) \frac{\beta_x \beta_y}{\beta^2} & 1 + (\gamma - 1) \frac{\beta_y^2}{\beta^2} & (\gamma - 1) \frac{\beta_y \beta_z}{\beta^2} \\ \beta_z \gamma & (\gamma - 1) \frac{\beta_x \beta_z}{\beta^2} & (\gamma - 1) \frac{\beta_y \beta_z}{\beta^2} & 1 + (\gamma - 1) \frac{\beta_z^2}{\beta^2} \end{pmatrix} \begin{pmatrix} m_1 + \epsilon \left(1 - \frac{m_1}{m_i}\right) \\ O(\sqrt{2\epsilon m_1}) \\ O(\sqrt{2\epsilon m_1}) \\ O(\sqrt{2\epsilon m_1}) \end{pmatrix} \quad (26)$$

for each $\vec{\beta} = \vec{\beta}_{1,2}$ which modifies (11) to

$$m_1' = \frac{\vec{p}_x}{\beta_{1x}\gamma_1 + \beta_{2x}\gamma_2 \pm O(\sqrt{2\epsilon/m_1})} \quad m_1'' = \frac{\vec{p}_y}{\beta_{1y}\gamma_1 + \beta_{2y}\gamma_2 \pm O(\sqrt{2\epsilon/m_1})} \quad (27)$$

The precise spread in the distribution of values of m_1 therefore depends on a convolution of the $\tilde{\chi}_i^0$ -velocity-distribution and three-body phase space, but from the above we can already see it is roughly of order $\sqrt{2\epsilon m_1}$.

References

- [1] H. Bachacou, I. Hinchliffe, and F. E. Paige, “Measurements of masses in SUGRA models at LHC.” *Phys.Rev.***D62**:015009 (2000); E. Lytken, “Derivation of some kinematical formulas in SUSY decay chains.” ATLAS note ATL-PHYS-COM-2004-001; J. M. Butterworth, J. Ellis and A. R. Raklev, “Reconstructing sparticle mass spectra using hadronic decays.” *JHEP* **0705**, 033 (2007); B.K. Gjelsten , D.J. Miller , and P. Osland. “Measurement of the gluino mass via cascade decays for SPS 1a.” *JHEP* **0506**:015 (2005); P. Huang, N. Kersting, and H.H. Yang, “Extracting MSSM Masses From Heavy Higgs Decays to Four Leptons at the LHC.” *Phys. Rev.* **D77**, 075011 (2008).
- [2] N. Kersting, work in progress.
- [3] B.C.Allanach et al., “The Snowmass points and slopes: Benchmarks for SUSY searches,” *Eur.Phys.J.***C25**,113-123 (2002).
- [4] G. Corcella *et al.*, *JHEP* **0101**: 010 (2001); S. Moretti, K. Odagiri, P. Richardson, M.H. Seymour and B.R. Webber, *JHEP* **0204**: 028 (2002).
- [5] J. Pumplin *et al.* (CTEQ Collaboration), *JHEP* **0207**:012 (2002);
D. Stump *et al.* (CTEQ Collaboration), *JHEP* **0310**:046 (2003);
- [6] G. Bian *et al.*, “Wedgebox analysis of four-lepton events from neutralino pair production at the LHC,” *Eur.Phys.J.***C53**, 429 (2008).

- [7] N. Kersting, “On Measuring Split-SUSY Gaugino Masses at the LHC,” arXiv:0806.4238 [hep-ph]
- [8] P. Huang, N. Kersting and H.H. Yang, “Extracting MSSM masses from heavy Higgs boson decays to four leptons at the CERN LHC,” Phys.Rev.**D77**, 075011 (2008).
- [9] M. Bisset, N. Kersting, and R. Lu, “Improving SUSY Spectrum Determinations at the LHC with Wedgebox and Hidden Threshold Techniques,” arXiv:0806.2492 [hep-ph].
- [10] K. Kawagoe, M. M. Nojiri and G. Polesello, “A new SUSY mass reconstruction method at the CERN LHC,” Phys.Rev.**D71**, 035008 (2005).
- [11] H.-C. Cheng *et al.*, “Mass determination in SUSY-like events with missing energy,” JHEP **0712**, 076 (2007).
- [12] C. G. Lester and D. J. Summers, “Measuring masses of semi-invisibly decaying particles pair produced at hadron colliders,” Phys.Lett.**B463**, 99 (1999); A. Barr, C. Lester and P. Stephens, “ $m(T_2)$: The truth behind the glamour,” J. Phys.**G29**, 2343 (2003).
- [13] W. S. Cho et al., “Measuring superparticle masses at hadron collider using the transverse mass kink,” JHEP **0802**, 035 (2008), Phys. Rev. Lett. **100**, 171801 (2008); A. J. Barr, B. Gripaios and C. G. Lester, “Weighing WIMPS with kinks at colliders: invisible particle mass measurements from endpoints,” JHEP **0802**, 014 (2008); M. M. Nojiri et al., “Inclusive transverse mass analysis for squark and gluino mass determination,” JHEP **0806**, 035 (2008).
- [14] A. Barr, G. G. Ross, and M. Serna, “The Precision Determination of Invisible-Particle Masses at the LHC,” Phys.Rev.**D78**, 056006 (2008).